A WRKY Transcription Factor Regulates Fe Translocation under Fe Deficiency[1][OPEN]

Jing Ying Yan, Chun Xiao Li, Li Sun, Jiang Yuan Ren, Gui Xin Li, Zhong Jie Ding*, and Shao Jian Zheng

State Key Laboratory of Plant Physiology and Biochemistry, College of Life Sciences, Zhejiang University, Hangzhou 310058, China (J.Y.Y., C.X.L., L.S., J.Y. R., Z.J.D., S.J.Z.); and College of Agronomy and Biotechnology, Zhejiang University, Hangzhou 310058, China (G.X.L.)

ORCID IDs: 0000-0003-1518-5143 (Z.J.D.); 0000-0002-3336-8165 (S.J.Z.).

Iron (Fe) deficiency affects plant growth and development, leading to reduction of crop yields and quality. Although the regulation of Fe uptake under Fe deficiency has been well studied in the past decade, the regulatory mechanism of Fe translocation inside the plants remains unknown. Here, we show that a WRKY transcription factor WRKY46 is involved in response to Fe deficiency. Lack of WRKY46 (*wrky46-1* and *wrky46-2* loss-of-function mutants) significantly affects Fe translocation from root to shoot and thus causes obvious chlorosis on the new leaves under Fe deficiency. Gene expression analysis reveals that expression of a nodulin-like gene (*VACUOLAR IRON TRANSPORTER1-LIKE1* [*VITL1*]) is dramatically increased in *wrky46-1* mutant. *VITL1* expression is inhibited by Fe deficiency, while the expression of *WRKY46* is induced in the root stele. Moreover, down-regulation of *VITL1* expression can restore the chlorosis phenotype on *wrky46-1* under Fe deficiency. Further yeast one-hybrid and chromatin immunoprecipitation experiments indicate that WRKY46 is capable of binding to the specific W-boxes present in the *VITL1* promoter. In summary, our results demonstrate that WRKY46 plays an important role in the control of root-to-shoot Fe translocation under Fe deficiency condition via direct regulation of *VITL1* transcript levels.

Iron (Fe) is an essential microelement for both plants and animals. Despite its abundance in the soil, Fe is only slightly soluble under aerobic conditions, especially in high-pH and calcareous soils, which results in Fe deficiency (Kobayashi and Nishizawa, 2012). Fe deficiency affects plant growth and development, leading to reduction of crop yield and quality, and causing health problems to human beings.

To cope with Fe deficiency, plants have developed two main strategies for Fe uptake. Except the graminеae, which use the strategy II mechanism to take up Fe from the soil, all other plants acquire Fe via strategy I mechanism (Schmidt, 2003). In strategy I, two main processes are involved, including the reduction of ferric chelates at the root surface and the absorption of the generated ferrous irons across the root plasma membrane (Kobayashi and Nishizawa, 2012). The dominant genes responsible for these processes were first cloned from Arabidopsis (*Arabidopsis thaliana*), known as the ferric-chelate reductase oxidase gene *FRO2* and the Fe-regulated transporter gene *IRT1* (Eide et al., 1996; Robinson et al., 1999). The expression of both genes is induced by Fe deficiency and is tightly regulated at multiple levels (Connolly et al., 2002, 2003; Barberon et al., 2011, 2014; Shin et al., 2013; Ivanov et al., 2014).

After acquisition of Fe from soils, plants transport the Fe from root epidermal cells to other tissues. Fe translocation in plants involves various steps, including radial transport across the root tissues, xylem loading and unloading, xylem-to-phloem transfer, phloem transport, symplastic movement toward the site of demand, and retranslocation from source or senescing tissue (Kobayashi and Nishizawa, 2012). Among these processes, xylem loading plays an essential role in root-to-shoot Fe translocation. A few transporter genes involved in xylem Fe loading have been isolated so far in Arabidopsis. *FERRIC REDUCTASE DEFFECTIVE3* (*FRD3*), encoding a member of MATE (multidrug and toxin efflux) transporter family, facilitates citrate efflux into xylem (Rogers and Guerinot, 2002; Durrett et al., 2007). Mutation of *FRD3* results in Fe localization to the central vascular cylinder of the roots and failure to transport it to aerial parts (Green and Rogers, 2004). Arabidopsis ferroportin1/iron regulated 1 (AtFPN1/AtIREG1), a potential novel effluxer, is expected to be responsible for free Fe transport into xylem, although the transport activity for IREG1 has not been reported (Morrissey et al., 2009). Besides, a group of nodulin-like genes, whose expression is dramatically down-regulated by Fe deficiency, show high similarity of protein

[1] This work was supported by the Natural Science Foundation of China (grant no. 31500206), the China Postdoctoral Science Foundation (grant no. 2015T80611), and the Fundamental Research Funds for the Central Universities.

* Address correspondence to zjding@zju.edu.cn.

The author responsible for distribution of materials integral to the findings presented in this article in accordance with the policy described in the Instructions for Authors (www.plantphysiol.org) is: Zhong Jie Ding (zjding@zju.edu.cn).

Z.J.D. and S.J.Z. designed the research; J.Y.Y., C.X.L., L.S., J.Y.R., G.X.L.; and Z.J.D. performed research; Z.J.D. and S.J.Z. analyzed data and contributed to writing the article.

[OPEN] Articles can be viewed without a subscription.

www.plantphysiol.org/cgi/doi/10.1104/pp.16.00252

sequence to AtVIT1 (vacuolar Fe uptake transporter 1; Kim et al., 2006) and are thought to function in Fe homeostasis in root vascular tissue, thus controlling the distribution of Fe between roots and shoots (Gollhofer et al., 2011, 2014). Nevertheless, little is known about the molecular regulatory mechanism of Fe translocation in plants.

Transcriptional regulation of Fe deficiency-responsive genes has been intensively studied in the past decade. The key regulator gene in Arabidopsis is *FIT1* (*Fe-DEFICIENCY INDUCED TRANSCRIPTION FACTOR1*, also known as *FIT/FRU/bHLH29*), which encodes a basic helix-loop-helix (bHLH) transcription factor (Colangelo and Guerinot, 2004). *FIT1* is indeed an ortholog of the tomato (*Solanum lycopersicum*) gene *FER* that is the first identified regulator of Fe deficiency responses in nongraminaceous plants (Ling et al., 2002). *FIT1* loss-of-function mutants show severe chlorosis and even die without excess Fe supply. While a great many Fe deficiency-inducible genes, including *IRT1* and *FRO2*, have significantly decreased expression in *fit1* mutant, it is not sufficient to induce the expression of these genes by only overexpressing *FIT1* under Fe supply (Colangelo and Guerinot, 2004). Yuan et al. (2008) further demonstrated that FIT1 needed another two bHLH proteins, bHLH38 or bHLH39, to activate the Fe deficiency responses. *bHLH38* and *bHLH39* belong to the subgroup Ib *bHLH* genes, together with *bHLH100* and *bHLH101* (Wang et al., 2007). These four *bHLH* genes function redundantly in Fe deficiency responses, and each of them can interact with *FIT1* at protein level (Wang et al., 2013). Furthermore, some other bHLH proteins, e.g. POPEYE (PYE) and its homologs, are capable of forming heterodimers and play an important role in the regulation of Fe homeostasis probably independent of *FIT1*-mediated signaling pathway (Long et al., 2010; Selote et al., 2015). This evidence reveals that the bHLH transcription factors have key roles in regulating Fe uptake and homeostasis in plants. Recently, the EIN3/EIL1 transcription factors in ethylene signaling pathway were shown to maintain FIT1 protein stability and enhance Fe deficiency response via interacting with FIT1 and the Mediator subunit MED16/25 complex (Lingam et al., 2011; Yang et al., 2014, 2016). Besides, two MYB transcription factors (MYB10/72) downstream of *FIT1* are also involved in Fe deficiency response by regulating expression of the nicotianamine synthase gene *NAS4* in Arabidopsis (Palmer et al., 2013). The question is raised if there is any other transcription factors involved in Fe deficiency responses.

WRKY proteins comprise one of the largest transcription factor families in plants (Eulgem et al., 2000). There are 72 WRKY members in Arabidopsis (Rushton et al., 2010). WRKY proteins contain one or two domains composed of the conserved amino acid sequence WRKYGQK, together with a zinc-finger-like motif (Ulker and Somssich, 2004). Using these domains, WRKYs can activate or repress transcription through directly binding to the W-box [core sequence: (T)(T)TGAC(C/T)] present in the promoters of target genes (Eulgem et al., 2000). WRKY transcription factors play important roles in a series of plant biological processes, including senescence, seed development, seed dormancy and germination, biotic and abiotic stress responses, etc. (Ulker and Somssich, 2004; Rushton et al., 2010). Recently, accumulating evidence has demonstrated that WRKY transcription factors also take part in the responses to nutritional stresses. For example, some WRKYs (WRKY6/42/45/75) regulate phosphate starvation responses in Arabidopsis (Devaiah et al., 2007; Chen et al., 2009; Wang et al., 2014; Su et al., 2015). Meanwhile, WRKY6 is involved in the response to boron deficiency (Kasajima et al., 2010). Another *WRKY* gene *WRKY46* functions negatively in resistance to aluminum stress (Ding et al., 2013).

Interestingly, there are a number of W-boxes present in the promoters of many Fe deficiency-responsive genes (e.g. *IRT1* and *NAS4*; Li et al., 2015), suggesting that WRKY transcription factor may play a role in Fe deficiency response. Here, we identified a *WKRY* gene, *WRKY46*, that is involved in the regulation of Fe translocation in Arabidopsis, through screening 72 *WRKYs* via gene expression and mutant analysis. WRKY46 has been reported to function in various processes, e.g. biotic and abiotic stress responses (Hu et al., 2012; Ding et al., 2013, 2014) and lateral root development (Ding et al., 2015), indicating WRKY46 as an important regulator in Arabidopsis. In this study, we discovered a previously unknown role for WRKY46 and demonstrated that WRKY46 promotes Fe translocation from root to shoot by suppressing the expression of a nodulin-like gene (*VIT1-like1*) under Fe deficiency.

RESULTS

WRKY46 Is Involved in Fe Deficiency Response

To evaluate the role of WRKY transcription factor in Fe deficiency response, we previously analyzed the expression pattern of *WRKY* genes that are present in the public microarray data sets under Fe deficiency treatment and found that five *WKRYs* are obviously induced by Fe deficiency (Supplemental Fig. S1). By further mutant analysis, we found that *wrky46* is more responsive to Fe deficiency than other *wrky* mutants. To confirm the role of WRKY46 in Fe deficiency response, we used two independent *WRKY46* T-DNA insertion mutant alleles, *wrky46-1* and *wrky46-2*, as previously described (Ding et al., 2013). Six-week-old wild-type and *wrky46* mutant plants grown in half-strength Murashige and Skoog (MS) nutrient solution were transferred into the same fresh solution with or without Fe supply for 6 d. There was no visible difference between the wild type and *wrky46* mutants on growth when sufficient Fe was supplied. However, in Fe free condition, the shoots, especially the new leaves of both *wrky46* mutants, were more chlorotic than those of the wild type (Fig. 1). This was also revealed by the corresponding SPAD (soil plant analysis development)

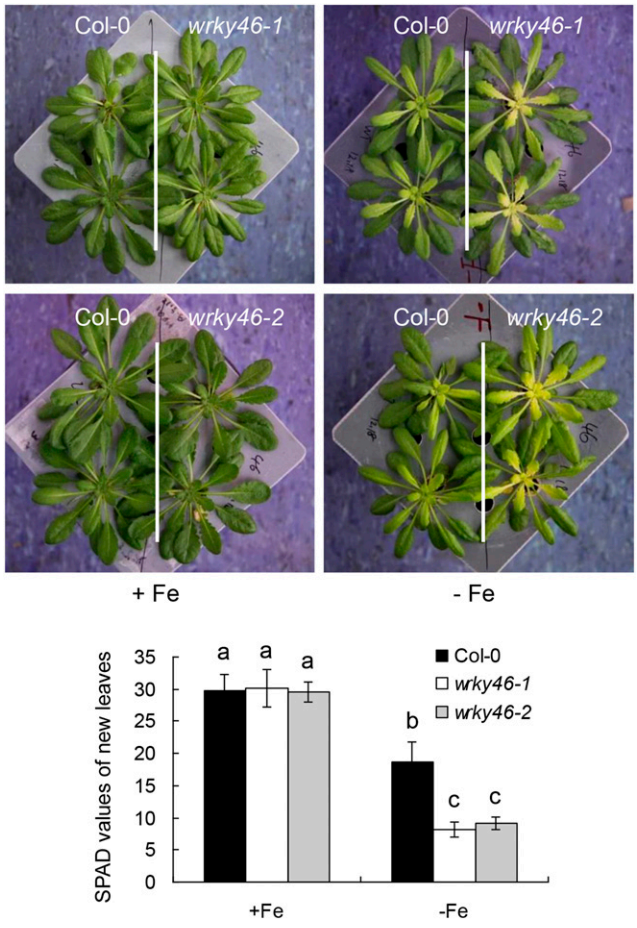

Figure 1. Lack of WRKY46 shows increased sensitivity to Fe deficiency. Growth of 6-week-old wild-type and *wrky46* loss-of-function mutant (*wrky46-1* and *wrky46-2*) plants under normal and Fe deficiency treatments for 6 d. The chlorophyll content or leaf greenness in the new leaves was indicated as SPAD values. Three independent experiments were done, each containing at least 10 plants per genotype for one treatment. Data were analyzed by one-way ANOVA following Duncan's test. Error bars with different letters represent a statistical difference ($P < 0.05$, Duncan's test).

values (Fig. 1), which indicate the chlorophyll content and leaf greenness. Actually, the leaves of *wrky46* mutants became obvious chlorotic after 3 d of Fe deficiency treatment, while the wild-type leaves showed slight chlorosis even after 5 d of treatment. To validate the function of WRKY46, we further performed experiments with a complemented *wrky46-1* mutant, which harbors a construct of *WRKY46pro:WRKY46-GFP* (as previously described; Ding et al., 2013). The complemented *wrky46-1* mutant plants displayed similar phenotypes to those of the wild type in both normal and Fe-deficient conditions (Supplemental Fig. S2). Taken together, these results indicate that *WRKY46* is involved in Fe deficiency response.

To verify if the expression of *WRKY46* is truly responsive to Fe deficiency, we detected the expression by RT-qPCR. It was evident that the transcript level of *WRKY46* was induced during different periods of Fe deficiency treatment (*IRT1* was used as a positive control; Fig. 2A). In accordance with this, the expression and activity of GUS driven by *WRKY46* native promoter were significantly increased in the root stele under Fe deficiency (Fig. 2, B and C). These results suggest that *WRKY46* expression is responsive to Fe deficiency.

WRKY46 Regulates Root-to-Shoot Fe Translocation

WRKY46 was previously demonstrated to modulate lateral root development under water stress via regulation of auxin levels in root (Ding et al., 2015). To confirm if the increased sensitivity of *wrky46* mutants to Fe deficiency results from the lack of lateral roots in the mutants, we compared the development of lateral roots in *wrky46* and wild-type plants and found that WRKY46 does not significantly affect lateral root development under Fe-deficient condition (Supplemental Fig. S3). Because auxin plays a potentially positive role in Fe deficiency responses (Chen et al., 2010), we also detected the effect of exogenous naphthylacetic acid (a permeable auxin analog) on Fe deficiency response of the wild type and *wrky46-1* and found that naphthylacetic acid could not obviously rescue chlorotic phenotype on *wrky46-1* mutant (Supplemental Fig. S4), which indicates that the increased sensitivity of *wrky46-1* to Fe

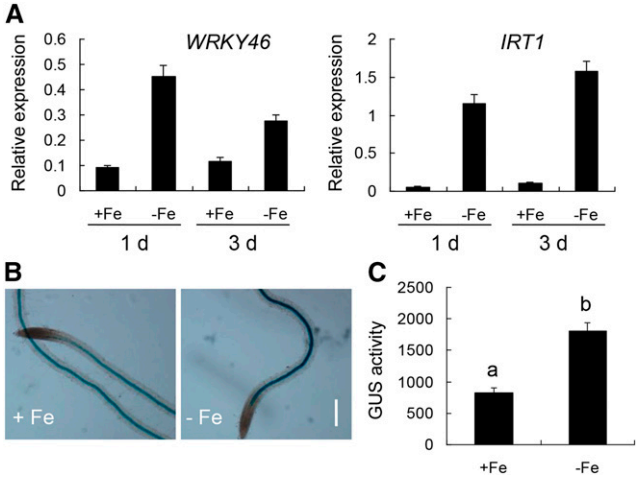

Figure 2. *WRKY46* expression is induced by Fe deficiency. A, Expression of *WRKY46* and *IRT1* in the wild type with or without Fe deficiency treatment. RNAs were extracted from roots of 6-week-old wild-type plants with or without Fe deficiency treatment for indicated days. Gene expression was determined by RT-qPCR using *ACT* mRNA as internal reference. B, Expression of *WRKY46* in roots via GUS staining without or with Fe deficiency treatment for 2 d. One-week-old transgenic plants carrying a $WRKY46_{pro}$:*GUS* construct were used for GUS staining. Bar = 100 μm. C, GUS activity measured in protein extracts from roots (in B) with or without Fe deficiency treatment. Activity units are given nmol methylumbelliferone (μg protein)$^{-1}$ min^{-1}. Three independent experiments were done. Data were analyzed by one-way ANOVA following Duncan's test. Error bars with different letters represent a statistical difference ($P < 0.05$, Duncan's test).

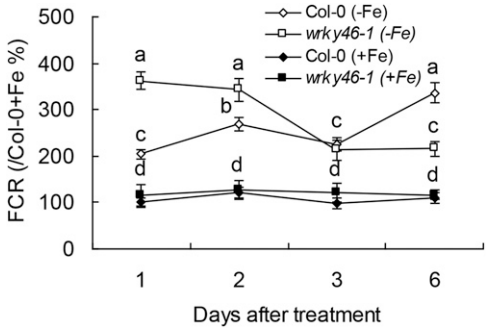

Figure 3. Effect of *WRKY46* on the induction of FCR activity under Fe deficiency. Relative FCR activity (the data of Col-0 + Fe at 1 d were set as 100%) of wild-type and *wrky46-1* mutant plants with or without Fe deficiency treatment for indicated days. Three independent experiments were done. Data were analyzed by one-way ANOVA following Duncan's test. Error bars with different letters represent a statistical difference ($P < 0.05$, Duncan's test).

deficiency might not be related to auxin homeostasis in roots. To further determine how WRKY46 controls responses to Fe deficiency, we analyzed ferric chelate reductase (FCR) activity, the typical indicator of Fe deficiency. Both the wild type and *wrky46-1* mutant increased FCR activity under different periods of Fe deficiency (versus Fe supplied condition; Fig. 3). There was no significant difference between the wild type and *wrky46-1* in FCR activity when Fe was sufficient, while under Fe deficiency conditions, *wrky46-1* had higher activity than the wild type under the first 2 d of treatment but had lower activity later at sixth day under Fe deficiency (Fig. 3). As *wrky46-1* mutant always shows obvious chlorosis after 3 d of Fe deficiency treatment, the effect of *wrky46* mutation on FCR activity thus seems to be more indirect.

To detect how WRKY46 contributes to Fe deficiency responses, we further measured Fe content in both wild-type and *wrky46-1* mutant plants with or without Fe supply. There was no significant difference between the wild type and *wrky46-1* mutants in Fe content in both roots and shoots when Fe was sufficient. However, *wrky46-1* mutants (versus the wild type) showed substantially higher Fe concentrations in roots but significantly lower in shoots under Fe deficiency (Fig. 4, A–C). Similarly, Perl staining revealed that *wrky46-1* mutants contained visibly elevated amounts of ferric Fe in their roots compared with wild-type plants (Supplemental Fig. S5A). This indicates that WRKY46 may play a role in Fe translocation from root to shoot. Consistent with this, the Fe content was dramatically lower in xylem sap of *wrky46-1* than in that of the wild type, especially under Fe deficiency (Fig. 4D).

Plants commonly contain elevated amounts of Zn and Mn under Fe-deficient conditions (Vert et al., 2002) because some Fe transporters (e.g. IRT1) nonspecifically take up or transport these metals. Interestingly, *wrky46-1* plants displayed decreased Zn and Mn levels in roots but increased that in shoots under both Fe-sufficient and -deficient conditions (Supplemental Fig. S5B), suggesting that the homeostasis of Zn and Mn is affected by altered translocation of Fe in *wrky46-1* mutant.

Besides, we also measured Fe concentrations in young leaves and old leaves separately and found that lack of WRKY46 does not significantly affect the

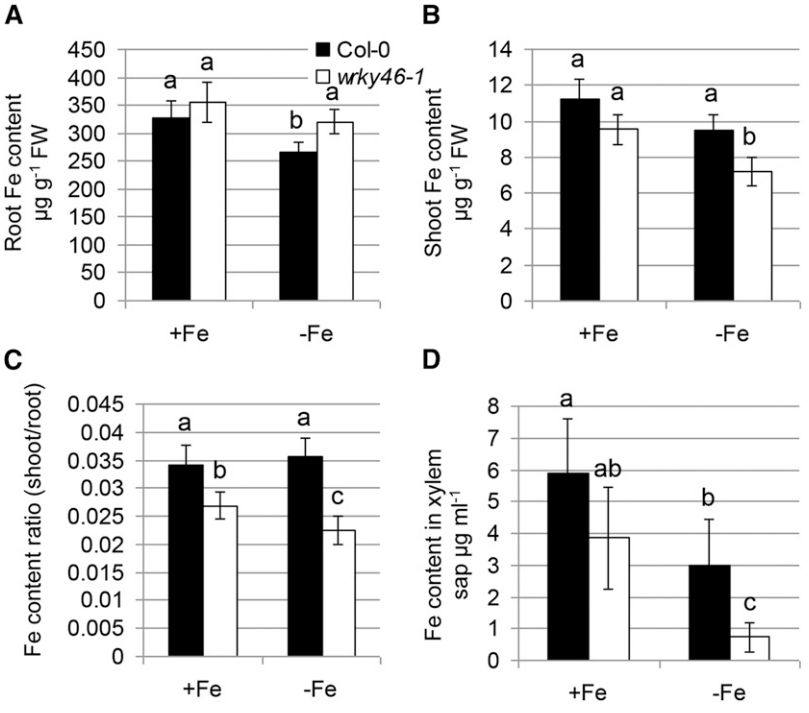

Figure 4. Lack of WRKY46 affects root-to-shoot Fe translocation. A and B, Fe content measured in roots (A) and shoots (B) of wild-type and *wrky46-1* mutant plants with or without Fe deficiency treatment for 6 d. C, The ratio of shoot Fe content (in B) to root Fe content (in A). D, Fe content in xylem sap of wild-type and *wrky46-1* mutant plants with or without Fe deficiency treatment. Three independent experiments were done. Data were analyzed by one-way ANOVA following Duncan's test. Error bars with different letters represent a statistical difference ($P < 0.05$, Duncan's test).

distribution of Fe between old and young leaves (Supplemental Fig. S6). Taken together, these results demonstrate that WRKY46 contributes to root-to-shoot Fe translocation under Fe-deficient conditions.

WRKY46 Regulates Expression of the Genes Involved in Fe Translocation

Previously, our microarray data revealed that the expression of two Fe translocation-related genes, *NICOTIANAMINE SYNTHASE2* (*NAS2*) and *VACUOLAR IRON TRANSPORTER1-LIKE1* (*VITL1*), was affected by *WRKY46* overexpression (Ding et al., 2014). *NAS2* encodes an enzyme that synthesizes nicotianamine and is responsible for Fe transport inside the body of plants (Schuler et al., 2012). *VITL1* encodes a potential Fe transporter involved in Fe uptake into vacuole (Gollhofer et al., 2014) and is proposed to function in Fe homeostasis in vascular tissues (Gollhofer et al., 2011). To confirm whether these two genes (*NAS2* and *VITL1*) are indeed regulated by WRKY46, we detected their expression in wild-type and *wrky46-1* mutant plants under Fe-sufficient or -deficient conditions. RT-qPCR data revealed that *NAS2* had obviously decreased expression in *wrky46-1* (versus the wild type) under both Fe-sufficient and -deficient conditions, while *VITL1* substantially increased expression in *wrky46-1* plants (Fig. 5). Moreover, we determined the expression of other Fe deficiency-responsive genes in wild-type and *wrky46-1* plants and found that most of these genes were not affected by loss of WRKY46 function, except *IRT1* and *FRO2*, whose expression was slightly increased in *wrky46-1* under Fe deficiency (Supplemental Figs. S7 and S8).

Lack of *VITL1* Rescues Responses of *wrky46-1* Mutant to Fe Deficiency

To verify if WRKY46 controls Fe translocation via the regulation of *NAS2* or *VITL1* expression, we first overexpressed *NAS2* in *wrky46-1* plants. The *NAS2/wrky46* transgenic plants, which harbor high expression levels of *NAS2*, showed similar phenotypes as those of *wrky46-1* mutants under Fe-deficient condition (Supplemental Fig. S9), indicating that *NAS2* does not dominantly contribute to the regulation of Fe deficiency response by WRKY46.

Next, we reduced the expression of *VITL1* on the *wrky46-1* mutant background using the RNA interference (RNAi) technique. The *VITL1-RNAi/wrky46* transgenic lines displayed less chlorotic than *wrky46-1* mutant plants under Fe deficiency at varying degrees, corresponding to the expression levels of *VITL1* in each line (Supplemental Fig. S10). The lowest expression of *VITL1* (in *VITL1-RNAi/wrky46-1* plants) restored the Fe-deficient phenotypes of *wrky46-1* mutant to that of the wild type (Fig. 6). These results suggest that *VITL1* is the major contributor to Fe translocation regulated by *WRKY46*.

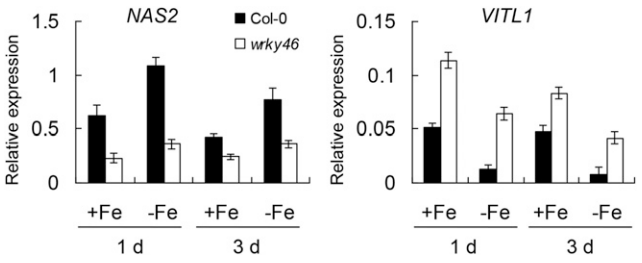

Figure 5. WRKY46 regulates the expression of Fe translocation genes. Expression of *NAS2* and *VITL1* in wild-type and *wrky46-1* mutant plants with or without Fe deficiency treatment. RNAs were extracted from roots of 6-week-old wild-type and *wrky46-1* mutant plants with or without Fe deficiency treatment for indicated days. Gene expression was determined by RT-qPCR using *ACT* mRNA as internal reference. Three independent repeats were done with similar results. Error bars indicate SD ($n = 3$).

WRKY46 Binds to the Promoter Region of *VITL1*

WRKY proteins recognize the W-boxes containing TTGACC/T core sequence present in the promoters of target genes. We found that there are three typical W-boxes in the *VITL1* promoter (2-kb region), suggesting that WRKY46 may regulate *VITL1* expression in a direct manner. To verify this possibility, three regions about 50 bp length surrounding each W-box, as shown in Figure 7, and the same regions with the mutant W-boxes were used as baits for binding assays in the yeast one-hybrid system (Fig. 7; Vidal and Legrain, 1999). The interactions between WRKY46 and these promoter fragments were tested by growth on media lacking Trp, Leu, and His. The His synthase inhibitor 3-aminotriazole (3AT) was added to the media to suppress background activation and assess the strength of the interaction. It was evident that yeast cotransformed with *WRKY46* and the natural promoter regions (VP1 and VP2), but not the corresponding mutant fragments (mVP1 and mVP2), grew well in the selective media (Fig. 7). Besides, yeast cotransformed with *WRKY46* and VP3 or mVP3 could not grow in the selective media. This indicates that WRKY46 is able to bind the specific regions (VP1 and VP2) in the *VITL1* promoter through the W-boxes.

We further performed chromatin immunoprecipitation (ChIP) analysis using the *WRKY46pro:WRKY46-GFP* transgenic line under Fe-sufficient and -deficient treatments (Ding et al., 2013) to determine whether WRKY46 directly binds to the *VITL1* promoter in vivo. After ChIP with anti-GFP antibody, the enrichment of specific *VITL1* promoter fragments in the immune precipitant was determined by qPCR using four primer pairs (VF1-4; Fig. 8). The normal mouse lgG and a specific *FIT1* promoter fragment containing the W-box were used as negative controls. We noticed that the VF2 region had a substantially stronger enrichment of WRKY46 than the negative controls, especially under Fe deficiency treatment, while VF1 and VF3 had little enrichment of WRKY46 (Fig. 8). These results suggest that WRKY46 regulates the expression of *VITL1* by binding to its promoter.

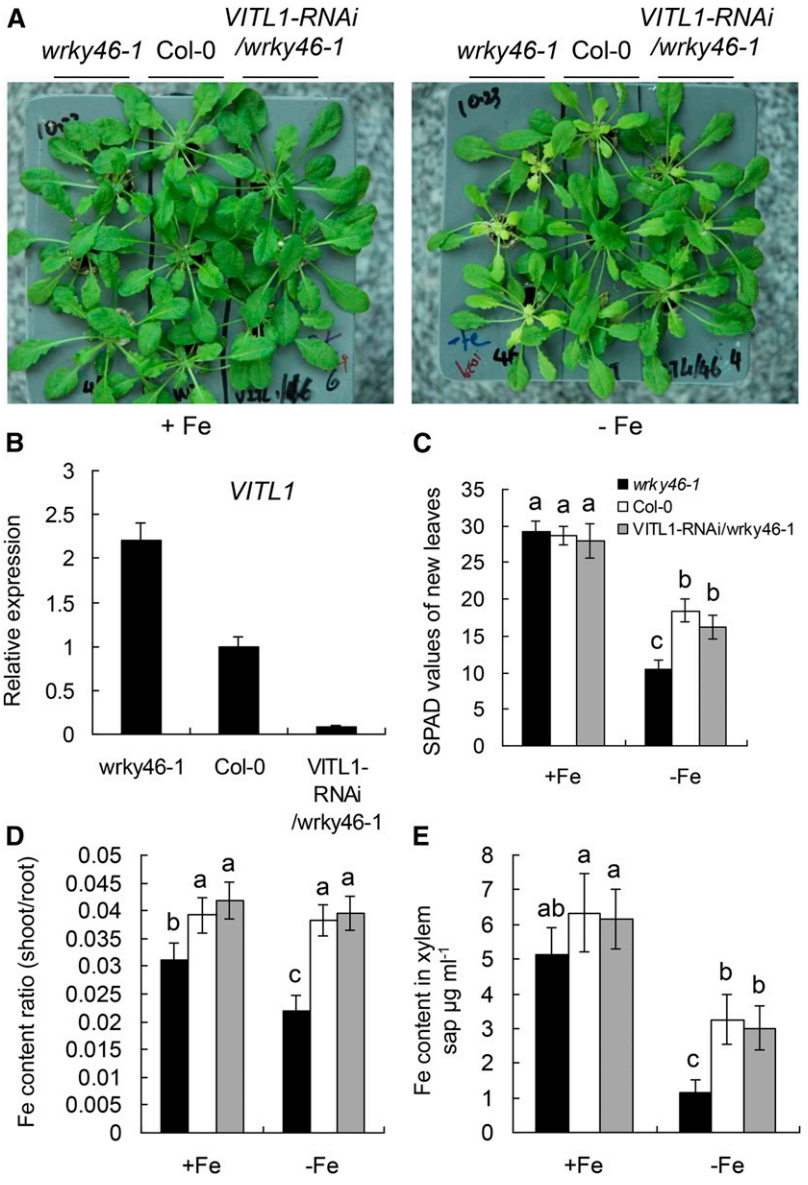

Figure 6. Loss of *VITL1* restores *wrky46-1* Fe deficiency phenotype. A, Growth of 6-week-old indicated genotypes with or without Fe deficiency treatment for 6 d. B, Expression of *VITL1* in roots of indicated genotypes. C, SPAD values of new leaves from indicated genotypes in A. D, Ratio of shoot-to-root iron content in indicated genotypes with or without Fe deficiency treatment (as in C). E, Fe content in xylem sap of indicated genotypes with or without Fe deficiency treatment. Three independent experiments were done. Data were analyzed by one-way ANOVA following Duncan's test. Error bars with different letters represent a statistical difference ($P < 0.05$, Duncan's test).

WRKY46 Acts Probably Independently of *FIT1- or PYE*-Mediated Signaling Pathway in Response to Fe Deficiency

The bHLH proteins, including FIT1 and PYE and their related bHLH transcription factors (e.g. bHLH38/39), have been considered as the key regulators of Fe uptake or homeostasis in Arabidopsis (Colangelo and Guerinot, 2004; Yuan et al., 2008; Long et al., 2010). Gene expression analysis revealed that the expression of *FIT1* (as well as other *bHLH* genes) was not affected by loss of WRKY46 function (Supplemental Fig. S7). To further investigate the relationship between *WRKY46* and *FIT1* or *PYE* signaling, we detected the transcript levels of *WRKY46* in the wild type, *fit1* loss-of-function mutant, the transgenic plants simultaneously overexpressing *FIT1* and *bHLH38* (OX29/38) or *FIT1* and b*HLH39* (OX29/39), and *pye-1* mutant plants under both Fe-sufficient and -deficient conditions. The qPCR revealed that *WRKY46* had similar expression levels in these genotypes (*fit1*, *OX29/38*, *OX29/39*, and *pye-1* versus the wild type; *IRT1* was used as a positive control; Supplemental Fig. S11). Taken together, these results suggest that WRKY46 may act independently of *FIT1* or *PYE* signaling in Fe deficiency responses.

DISCUSSION

Fe is an essential micronutrient for plants, and its acquisition is tightly controlled, as both deficient and excess Fe are pernicious for plants to grow and develop. The bHLH protein-dependent transcriptional regulation (FIT1- and PYE-dependent) plays a key role in the control of Fe uptake and homeostasis in plants (Colangelo and Guerinot, 2004; Long et al., 2010; Selote et al., 2015). Here, we show another kind of transcription factor that is from WRKY family participating in Fe deficiency response in Arabidopsis.

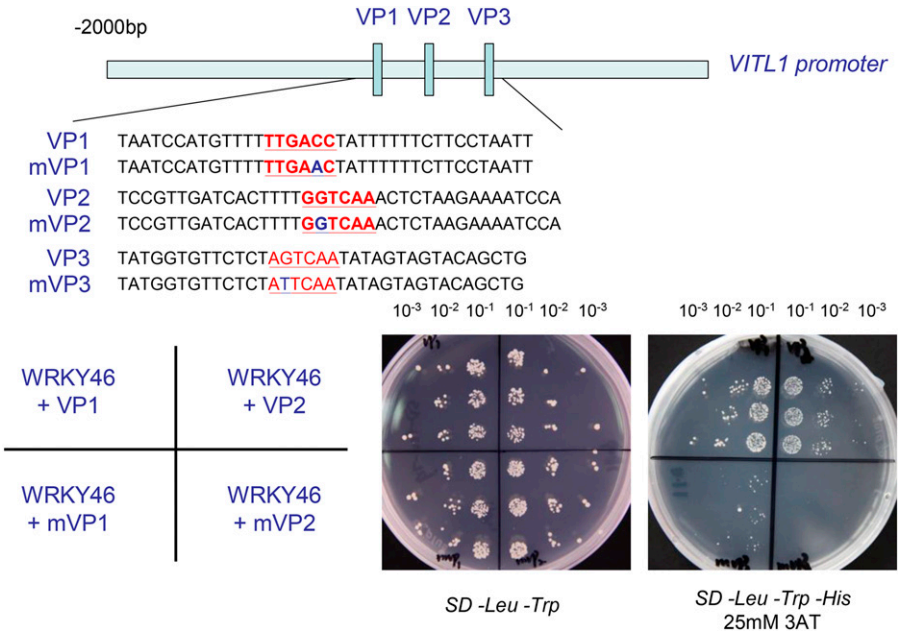

Figure 7. WRKY46 binds to *VITL1* promoter region in yeast. The 2-kb promoter region of *VITL1* was indicated. The small blue boxes in the promoter represent three W-boxes (corresponding to the sequences in red). VP1-3 indicate the promoter fragments (about 50 bp) surrounding each W-box, and mVP1-3 indicate the mutated VP1-3 (with 1 bp mutation in each W-box), respectively. Yeast cells were cotransformed with a bait vector, containing a promoter fragment (VP1-3 and mVP1-3) fused to a *HIS2* reporter gene, and a prey vector, containing *WRKY46* fused to a *GAL4* activation domain. Cells were grown in liquid media to OD_{600} of 0.1 (10^{-1}) and diluted in a 10× dilution series (10^{-2} to 10^{-3}). Of each dilution, 5 μL was spotted on media selecting for both plasmids (SD –Trp –Leu) and selecting for interaction (SD –Trp –Leu –His), supplemented with 25 mM 3AT to suppress background growth and test the strength of the interaction.

WRKY transcription factors have important roles in various plant biological processes, including developmental regulation and stress responses (Rushton et al., 2010). Accumulating evidence reveals that *WRKY* genes are also involved in plant responses to nutrient deficiency or toxicity. For example, a number of WRKYs regulate phosphate uptake and translocation in Arabidopsis (Devaiah et al., 2007; Chen et al., 2009; Wang et al., 2014; Su et al., 2015). Interestingly, W-boxes, the DNA binding sites of WRKY proteins, are enriched in the promoters of many Fe deficiency-responsive genes (Li et al., 2015). Although some rice (*Oryza sativa*) *WRKY* genes may play a role in response to Fe excess stress possibly through responding to disturbed redox homeostasis (Ricachenevsky et al., 2010), little is known about whether WRKY proteins take part in Fe deficiency responses. Among total *WRKY* genes present in public microarray data, there are five *WRKYs* that are responsive to Fe deficiency at transcript levels (Supplemental Fig. S1), including *WRKY46*. Our preliminary mutant analysis revealed that the *wrky46* loss-of-function mutants show obvious chlorosis other than other *wrky* mutants under Fe deficiency conditions, indicating that *WRKY46* may function specifically or have less redundancy with other *WRKYs* in Fe deficiency response. Further using independent *wrky46* knockout mutants as well as the complemented *wrky46-1* transgenic lines, we confirmed the response of *WRKY46* to Fe deficiency (Fig. 1; Supplemental Fig. S2).

FCR activity is a typical indicator of Fe deficiency (Yi and Guerinot, 1996). Because the mutants lacking *WRKY46* generally show visible chlorosis on new leaves in 3 d of Fe deficiency treatment, together with the evidence that *WRKY46* is expressed in root stele (Fig. 2), the mutants displaying higher FCR activity (versus the wild type) at the early Fe deficiency treatment (for 1 and 2 d; Fig. 3) may suggest that Fe deficiency is more severe in the mutants during these periods and that lack of WRKY46 function has an indirect effect on FCR activity as well as on Fe uptake processes. Accordingly, the expression of Fe uptake related genes (*IRT1* and *FRO2*) is higher in *wrky46* mutants (versus the wild type; Supplemental Fig. S7). This can also be found in other Fe deficiency-responsive mutants. For example, *frd3* mutants that are defective in Fe translocation from root to shoot resulted from the failure of loading of citrate into xylem (Green and

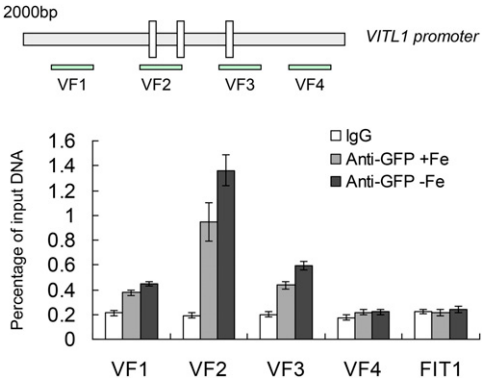

Figure 8. WRKY46 binds to *VITL1* promoter in vivo. Diagram of *VITL1* promoter showing three W-boxes. VF1-4 indicate genomic DNA fragments around the *VITL1* promoter for ChIP assay. ChIP analysis showing the direct binding of WRKY46 to the VITL1 promoter in vivo. Eight-day-old *WRKY46pro-WRKY46-GFP* transgenic seedlings with or without Fe deficiency treatment were used for ChIP analysis. The IgG and a fragment of *FIT1* promoter were used as negative controls. Three independent repeats were done with similar results. Error bars indicate SD ($n = 3$).

Rogers, 2004) have higher levels of Fe deficiency responses (including FCR activity) under both Fe-sufficient and -deficient conditions (Rogers and Guerinot, 2002; Durrett et al., 2007). However, *wrky46-1* mutants show a lower FCR activity than the wild type at the sixth day following onset of Fe deficiency treatment (Fig. 3), which might be due to more seriously secondary effects raised by long-term exposure to Fe deficiency stress in the mutants, although we can't rule out the possibility that WRKY46 regulates Fe uptake in a non-cell-autonomous way.

Further analysis revealed that *wrky46-1* mutants showed lower ratios of shoot-to-root Fe content (versus the wild type; Fig. 4, A–C) and that Fe concentrations in xylem sap were significantly lower in the mutants lacking *WRKY46* than in the wild type (Fig. 4D). This suggests that *wrky46* mutant plants had decreased capacity of root-to-shoot Fe translocation, which was potentially caused by the reduced loading of iron into the xylem in the mutants, thus indicating a role of *WRKY46* in promoting root Fe transport to shoot. Furthermore, the content of other divalent metals (e.g. Zn and Mn) increased in shoots and decreased in roots, which was opposite to the change of Fe content in *wrky46-1* mutants (versus the wild type; Supplemental Fig. S5B). Since the concentrations of these metals can efficiently reflect the Fe nutritional status (Baxter et al., 2008), such altered homeostasis of these metals (Zn and Mn) thereby again supported the contribution of *WRKY46* to Fe translocation from root to shoot. But unlike in other research (Vert et al., 2002; Long et al., 2010), the total content of Zn and Mn (in whole plant) was not significantly increased in *wrky46-1* mutants (versus the wild type) under Fe deficiency (Supplemental Fig. S5B). This might be because Fe deficiency in *wrky46-1* was not severe enough to induce higher expression levels of *IRT1* that is responsible for nonselective uptake of different kind of divalent metals in addition to Fe (Supplemental Fig. S7; Vert et al., 2002), thus making it unable to accumulate more non-Fe metals in *wrky46* plants. Besides, the expression of *WRKY46* in root stele also favors our conclusion that WRKY46 is involved in regulation of root-to-shoot Fe translocation under Fe-deficient condition (Fig. 2).

A small family of nodulin-like genes (including *VITL1*) that are induced by elevated Fe concentrations at transcript levels while inhibited by Fe deficiency encode putative cationic metal transporters and are thought to function in Fe homeostasis to protect plants from excess Fe stress (Gollhofer et al., 2011). Lack of some of these genes (e.g. *Nodulin-like3/21*) increased the ratios of shoot-to-root Fe content, suggesting that these nodulin-like genes are probably involved in Fe distribution between shoots and roots (Gollhofer et al., 2011). VITL1 (also named Nodulin-like1) localized to the vacuolar membrane and is responsible for Fe uptake into vacuoles (Gollhofer et al., 2011, 2014). We speculate that *VITL1* is the major contribution to the root-to-shoot Fe translocation regulated by WRKY46. First, the transcript levels of *VITL1* are obviously elevated in *wrky46-1* mutants (versus the wild type) under both Fe-sufficient and -deficient conditions, and Fe deficiency inhibits *VITL1* expression dramatically in the wild type but less in the mutants (Fig. 5). Consistent with this, *WRKY46* is induced by Fe deficiency at transcript level, whereas *VITL1* is down-regulated (Figs. 2 and 5; Gollhofer et al., 2011). Second, both *WRKY46* and *VITL1* are expressed in root stele as well as in vasculature tissues in shoots (Fig. 2; Gollhofer et al., 2011; Ding et al., 2014), suggesting they have similar expression patterns. Third, down-regulation of *VITL1* significantly increases Fe concentrations in xylem sap of *wrky46* mutants and thus restores Fe homeostasis and Fe deficiency response of *wrky46* mutants to that of the wild type (Fig. 6), indicating that *VITL1* is epistatic to *WRKY46* in response to Fe deficiency. Finally, the yeast one-hybrid experiment and ChIP assay reveal that WRKY46 can bind to the promoter of *VITL1* through specific W-boxes (Figs. 7 and 8), suggesting the regulation of *VITL1* by WRKY46 is in a direct manner.

In summary, we established a role for *WRKY46* in Fe deficiency responses. We present that WRKY46 is induced under Fe-deficient conditions and that it directly inhibits the transcription of *VITL1*, which is responsible for transport of iron into vacuoles in the root stele cells, thus promoting root-to-shoot Fe translocation by releasing more iron into root xylem. The function of WRKY46 is probably independent of the well-known bHLH transcription factors (FIT and PYE; Supplemental Fig. S11), suggesting that WRKY46 may contribute to another signaling pathway to complement the bHLH protein-mediated Fe deficiency responses. In addition, it's interesting to find that *WRKY46* expression is inhibited by aluminum stress (Ding et al., 2013), but induced by Fe deficiency (as shown in this article). This seems to be evolutionarily reasonable, as both of the stresses are present in the different kind of soil conditions respectively: Aluminum stress exists in acidic soils, while Fe deficiency usually can be seen in basic soils. It is economical and advisable for plants to have such genes (e.g. *WRKY46*) that simultaneously control multiple biological processes, making them adaptive to variable environments.

MATERIALS AND METHODS

Plant Materials and Growth Conditions

Arabidopsis (*Arabidopsis thaliana*) plants were grown in a controlled environment growth room programmed for a 12-h-light/12-h-dark cycle with a constant temperature of 22°C. T-DNA insertion mutants *wrky46-1* (SAIL_1230_H01) and *wrky46-2* (SALK_134310C) were used as previously described (Ding et al., 2013). The *fit1* mutants and OX29/38-5 and OX29/39-12 transgenic lines were obtained from Prof. Hongqing Lin (Institute of Genetics and Developmental Biology, Chinese Academy of Sciences). *pye-1* T-DNA insertion mutants (SALK_021217) were obtained from the ABRC. *WRKY46*$_{pro}$*:WRKY46-GFP* was transformed into *wrky46-1* plants, and *WRKY46*$_{pro}$*:GUS* were transformed into wild-type (Col-0) plants, respectively (Ding et al., 2013). *35S:NAS2* was constructed in pCambia1301 vector; for *VITL1-RNAi* construction, the specific

DNA fragments from *VITL1* were first subcloned into pAGRIKOLA vector and then constructed into pCambia1301 vector driven by *35S* promoter. Both of the *35S:NAS2* and *VITL1-RNAi* constructs were further transformed into *wrky46-1* mutant plants through *Agrobacterium tumefaciens* GV3101, and homozygous lines were selected via screening on media containing hygromycin B and via further PCR-based confirmation. All genotypes used in this study have the Col-0 genetic background.

Plants were grown on modified half-strength MS agar medium or solution (pH 5.6) as described previously (Ding et al., 2014). For hydroponic Fe deficiency treatment, 6-week-old various genotypes grown in half-strength MS nutrient solution were transferred into the same fresh solution with or without Fe supply for different periods (3–6 d). The nutrient solution was changed every 2 d. For Fe deficiency treatment on agar plates, 3- to 8-d-old seedlings grown on half-strength MS medium were transferred onto the same fresh medium containing 300 μM ferrozine (an Fe chelator) for the indicated days of treatment.

Chlorophyll Content Analysis

Chlorophyll content was expressed in terms of SPAD value, which was determined on the fully expanded youngest leaves of seedlings with a portable chlorophyll meter (Konica Minolta SPAD-502).

FCR Activity Measurement

FCR activity was determined according to Lei et al. (2014). Briefly, whole excised roots were placed into a falcon tube filled with 20 mL of assay solution consisting of 0.5 mM $CaSO_4$, 0.1 mM 4-morpho-lineethanesulfonic acid, 0.1 mM bathophenanthroline-disulfonic acid disodium salt hydrate (BPDS), and 100 mM Fe- EDTA at pH 5.5, adjusted with 1 M NaOH. The tubes were placed on a shaker (60 rpm) in a dark room at 25°C for 1 h. The absorbance of the assay solutions was recorded by a spectrophotometer (Shimadzu) at 535 nm, and the concentration of Fe(II)$[BPDS]_3$ was calculated using an extinction coefficient of 22.14 mM^{-1} cm^{-1}. The data were expressed as the means of relative root FCR activity.

Perl Staining

Perl's staining for Fe^{3+} localization was performed according to Long et al. (2010). Briefly, 7-d-old seedlings grown on sufficient media were vacuum infiltrated with Perl's stain solution (equal volumes of 4% [v/v] HCl and 4% [w/v] K-ferrocyanide) for 30 min. Seedlings were then incubated for another 30 min in Perl staining solution, washed three times with water, observed, and photographed with a stereoscope (Nikon) equipped with a CCD camera.

Fe Content Determination

Roots and shoots from treated plants were harvested separately, washed three times with ddH_2O, weighed, and digested with HNO_3:$HClO_4$ (4:1, v/v). The total Fe concentrations were determined by inductively coupled plasma-atomic emission spectrometry (ICP optical emission spectrometry). The young leaves were indicated as half the number of total leaves that were counted outward from the center of the rosette. The rest of the rosette leaves were indicated as old leaves.

Xylem Sap Collection and Fe Content Measurement

Xylem sap was collected by excision of the hypocotyls below the rosette with a sharp scalpel as previously described (Schuler et al., 2012). The first droplet was discarded to minimize possible contamination. Then, a pipette tip (1–10 μL size) was carefully mounted over the stem and xylem sap was subsequently soaked into the mounted pipette tip due to capillary forces. The collection was carried out for 30 min, and the total volume was determined. Collected sap samples were later diluted in 5% HNO_3 solution, and the Fe content was determined by ICP-OES.

GUS Analysis

GUS staining of 1-week-old transgenic lines with or without Fe deficiency treatment (on plate) for 2 d was performed by immersing seedlings in a staining solution [100 mM sodium-phosphate buffer, pH 7, 2 mM $K_4Fe(CN)_6$, 2 mM $K_3Fe(CN)_6$, 0.2% Triton X-100, 10 mM EDTA, and 2 mM X-Gluc] in a 10-mL tube for 12 h at 37 in the dark followed by two times washes with 70% ethanol to remove chlorophyll. Samples were photographed using a stereoscope (Nikon) equipped with a CCD camera.

For GUS activity quantification, the seedlings with or without Fe deficiency treatment for 2 d were collected and lysed for assays in a extraction buffer (50 mM NaH_2PO_4, pH 7.0, 10 mM EDTA, 0.1% Triton X-100, 0.1% sodium lauryl sarcosine, and 10 mM β-mercaptoethanol) by freezing with liquid nitrogen and grinding with mortar and pestle. The GUS activity assay was performed using the substrate 4-methylumbelliferyl glucuronide (Sigma-Aldrich) and the standards of methylumbelliferone (Sigma-Aldrich) as previously described (Jefferson et al., 1987).

Gene Expression Analysis

For real-time qPCR, total RNAs from roots of various genotypes were extracted using the RNAprep pure Plant Kit (from TianGen Biotech Co. of Qiagen) according to the manufacturer's protocol. Total RNAs treated with DNase I (TianGen Biotech Co. of Qiagen) were converted into cDNAs using the PrimeScript RT reagent kit (Takara). Real-time qPCR analysis was carried out using the SYBR Premix Ex Taq II (Takara) on a Roche LightCycler480 real-time qPCR system, following the manufacturer's instructions. Transcript levels of each mRNA were determined and normalized with the level of *ACT* mRNAs using the delta Ct method (Czechowski et al., 2005; Schmittgen and Livak, 2008). Gene-specific primers are listed in Supplemental Table S1.

The expression browser tool provided by BAR (The BioArray Resource for Arabidopsis Functional Genomics; http://bbc.botany.utoronto.ca/; Toufighi et al., 2005) was employed to show the heat map of gene expression patterns in Supplemental Figure S1.

Yeast One-Hybrid Experiments

WRKY46 coding regions were amplified and cloned into the pGADT7-rec2 prey vector (Clontech), creating a translational fusion between the GAL4 activation domain and the transcription factor. For construction of the pHIS2 vector, forward and reverse oligonucleotides (Fig. 7) were annealed, digested by *Eco*RI/*Sac*I, and subcloned into *Eco*RI/*Sac*I-linearized pHIS2 vector. Competent yeast cells were prepared according to the Clontech Yeast Protocols Handbook using the Y187 yeast strain. For yeast transformation, 50 μL of competent yeast cells were incubated with 100 ng of pHIS2 bait vector and 100 ng of pGADT7-Rec2 prey vector, 50 μg salmon sperm Carrier DNA (Invitrogen), and 0.5 mL PEG/LiAc solution. Cells were transformed according to the manufacturer's instructions. Transformations were plated onto SD media –Leu –Trp to select for cotransformed cells and incubated at 28°C for 4 d. Transformed yeast cells were subsequently grown in SD –Trp –Leu liquid media to OD_{600} of 0.1 and diluted in a 10× dilution series. From each dilution, 5 μL was spotted on SD –Trp –Leu and on SD –Trp –Leu –His media plates supplemented with 25 mM 3AT (Sigma-Aldrich). The plates were then incubated for 3 d at 28°C.

ChIP Assay

The EpiQuik Plant ChIP kit (Epigentek) was used to perform the ChIP assays. In brief, 0.8 to 1.0 g of 8-d-old *Pro-46-WRKY46-sGFP* seedlings with or without Fe deficiency treatment (on plate) for 2 d were fixed with 20 mL of 1.0% formaldehyde by vacuuming for 10 min. The chromatin DNA was extracted and sheared to 200- to 1000-bp fragments by sonicating. One hundred microliters of the sheared DNA was immunoprecipitated with 3 to 5 μg anti-GFP (Abcam) for 90 min at 50 to 100 rpm at room temperature. In addition, 1 μL of normal mouse IgG (Epigentek) was used as a negative control. DNA fragments that specifically associated with WRKY46 were released, purified, and used as templates for real-time qPCR using specific primers (Supplemental Table S1).

Accession Numbers

Sequence data from this article can be found in the GenBank/EMBL data libraries under the following accession numbers: WRKY46 (At2g46400), VITL1 (At1g21140), IRT1 (At4g19690), FRO2 (At1g01580), FIT1 (At2g28160), bHLH38 (At3g56970), bHLH39 (At3g56980), bHLH100 (At2g41240), bHLH101 (At5g04150), PYE (At3g47640), FRD3 (At3g08040), NAS1 (At5g04950), NAS2 (At5g56080), NAS4 (At1g56430), YSL1 (At4g24120), YSL2 (At5g24380),

NRAMP3 (At2g23150), NRAMP4 (At5g67330), IREG1 (At2g38460), Nodulin-like2 (At1g76800), Nodulin-like3 (At3g43630), Nodulin-like4 (At3g43660), and Nodulin-like21 (At3g25190).

Supplemental Data

The following supplemental materials are available.

Supplemental Figure S1. Expression pattern of *WRKY* genes in response to Fe deficiency revealed by BAR Expression Browser.

Supplemental Figure S2. Lack of WRKY46 affects sensitivity to Fe deficiency.

Supplemental Figure S3. Lack of WRKY46 does not significantly affect lateral root development in Fe deficiency condition.

Supplemental Figure S4. Auxin cannot rescue response of *wrky46-1* to Fe deficiency.

Supplemental Figure S5. Microelements content analysis in wild-type and *wrky46-1* mutant plants.

Supplemental Figure S6. WRKY46 does not significantly affect old to young leaves in Fe translocation.

Supplemental Figure S7. Expression analysis of Fe deficiency-responsive genes in wild-type and *wrky46-1* mutant plants.

Supplemental Figure S8. Expression of nodulin-like genes in wild-type and *wrky46-1* mutant plants.

Supplemental Figure S9. Increased expression of *NAS2* can't restore Fe deficiency phenotype on *wrky46-1* mutant.

Supplemental Figure S10. Lack of VITL1 rescues *wrky46-1* sensitivity to Fe deficiency.

Supplemental Figure S11. *WRKY46* expression is not regulated by FIT1 or PYE transcription factors.

Supplemental Table S1. Primers used in this study.

ACKNOWLEDGMENTS

We thank Prof. HongQing Lin (Institute of Genetics and Developmental Biology, Chinese Academy of Sciences) for kindly providing the *fit1* mutant and OX29/38-5 and OX29/39-12 transgenic line seeds.

Received February 17, 2016; accepted May 14, 2016; published May 19, 2016.

LITERATURE CITED

Barberon M, Dubeaux G, Kolb C, Isono E, Zelazny E, Vert G (2014) Polarization of IRON-REGULATED TRANSPORTER 1 (IRT1) to the plant-soil interface plays crucial role in metal homeostasis. Proc Natl Acad Sci USA **111:** 8293–8298

Barberon M, Zelazny E, Robert S, Conéjéro G, Curie C, Friml J, Vert G (2011) Monoubiquitin-dependent endocytosis of the iron-regulated transporter 1 (IRT1) transporter controls iron uptake in plants. Proc Natl Acad Sci USA **108:** E450–E458

Baxter IR, Vitek O, Lahner B, Muthukumar B, Borghi M, Morrissey J, Guerinot ML, Salt DE (2008) The leaf ionome as a multivariable system to detect a plant's physiological status. Proc Natl Acad Sci USA **105:** 12081–12086

Chen WW, Yang JL, Qin C, Jin CW, Mo JH, Ye T, Zheng SJ (2010) Nitric oxide acts downstream of auxin to trigger root ferric-chelate reductase activity in response to iron deficiency in Arabidopsis. Plant Physiol **154:** 810–819

Chen YF, Li LQ, Xu Q, Kong YH, Wang H, Wu WH (2009) The WRKY6 transcription factor modulates PHOSPHATE1 expression in response to low Pi stress in Arabidopsis. Plant Cell **21:** 3554–3566

Colangelo EP, Guerinot ML (2004) The essential basic helix-loop-helix protein FIT1 is required for the iron deficiency response. Plant Cell **16:** 3400–3412

Connolly EL, Fett JP, Guerinot ML (2002) Expression of the IRT1 metal transporter is controlled by metals at the levels of transcript and protein accumulation. Plant Cell **14:** 1347–1357

Connolly EL, Campbell NH, Grotz N, Prichard CL, Guerinot ML (2003) Overexpression of the FRO2 ferric chelate reductase confers tolerance to growth on low iron and uncovers posttranscriptional control. Plant Physiol **133:** 1102–1110

Czechowski T, Stitt M, Altmann T, Udvardi MK, Scheible WR (2005) Genome-wide identification and testing of superior reference genes for transcript normalization in Arabidopsis. Plant Physiol **139:** 5–17

Devaiah BN, Karthikeyan AS, Raghothama KG (2007) WRKY75 transcription factor is a modulator of phosphate acquisition and root development in Arabidopsis. Plant Physiol **143:** 1789–1801

Ding ZJ, Yan JY, Xu XY, Li GX, Zheng SJ (2013) WRKY46 functions as a transcriptional repressor of *ALMT1,* regulating aluminum-induced malate secretion in *Arabidopsis.* Plant J **76:** 825–835

Ding ZJ, Yan JY, Xu XY, Yu DQ, Li GX, Zhang SQ, Zheng SJ (2014) Transcription factor WRKY46 regulates osmotic stress responses and stomatal movement independently in *Arabidopsis.* Plant J **79:** 13–27

Ding ZJ, Yan JY, Li CX, Li GX, Wu YR, Zheng SJ (2015) Transcription factor WRKY46 modulates the development of Arabidopsis lateral roots in osmotic/salt stress conditions via regulation of ABA signaling and auxin homeostasis. Plant J **84:** 56–69

Durrett TP, Gassmann W, Rogers EE (2007) The FRD3-mediated efflux of citrate into the root vasculature is necessary for efficient iron translocation. Plant Physiol **144:** 197–205

Eide D, Broderius M, Fett J, Guerinot ML (1996) A novel iron-regulated metal transporter from plants identified by functional expression in yeast. Proc Natl Acad Sci USA **93:** 5624–5628

Eulgem T, Rushton PJ, Robatzek S, Somssich IE (2000) The WRKY superfamily of plant transcription factors. Trends Plant Sci **5:** 199–206

Gollhofer J, Schläwicke C, Jungnick N, Schmidt W, Buckhout TJ (2011) Members of a small family of nodulin-like genes are regulated under iron deficiency in roots of *Arabidopsis thaliana*. Plant Physiol Biochem **49:** 557–564

Gollhofer J, Timofeev R, Lan P, Schmidt W, Buckhout TJ (2014) Vacuolar-Iron-Transporter1-Like proteins mediate iron homeostasis in Arabidopsis. PLoS One **9:** e110468

Green LS, Rogers EE (2004) FRD3 controls iron localization in Arabidopsis. Plant Physiol **136:** 2523–2531

Hu Y, Dong Q, Yu D (2012) Arabidopsis WRKY46 coordinates with WRKY70 and WRKY53 in basal resistance against pathogen *Pseudomonas syringae.* Plant Sci **185-186:** 288–297

Ivanov R, Brumbarova T, Blum A, Jantke A-M, Fink-Straube C, Bauer P (2014) SORTING NEXIN1 is required for modulating the trafficking and stability of the Arabidopsis IRON-REGULATED TRANSPORTER1. Plant Cell **26:** 1294–1307

Jefferson RA, Kavanagh TA, Bevan MW (1987) GUS fusions: β-glucuronidase as a sensitive and versatile gene fusion marker in higher plants. EMBO J **6:** 3901–3907

Kasajima I, Ide Y, Yokota Hirai M, Fujiwara T (2010) WRKY6 is involved in the response to boron deficiency in *Arabidopsis thaliana.* Physiol Plant **139:** 80–92

Kim SA, Punshon T, Lanzirotti A, Li L, Alonso JM, Ecker JR, Kaplan J, Guerinot ML (2006) Localization of iron in Arabidopsis seed requires the vacuolar membrane transporter VIT1. Science **314:** 1295–1298

Kobayashi T, Nishizawa NK (2012) Iron uptake, translocation, and regulation in higher plants. Annu Rev Plant Biol **63:** 131–152

Lei GJ, Zhu XF, Wang ZW, Dong F, Dong NY, Zheng SJ (2014) Abscisic acid alleviates iron deficiency by promoting root iron reutilization and transport from root to shoot in Arabidopsis. Plant Cell Environ **37:** 852–863

Li H, Wang L, Yang ZM (2015) Co-expression analysis reveals a group of genes potentially involved in regulation of plant response to iron-deficiency. Gene **554:** 16–24

Lingam S, Mohrbacher J, Brumbarova T, Potuschak T, Fink-Straube C, Blondet E, Genschik P, Bauer P (2011) Interaction between the bHLH transcription factor FIT and ETHYLENE INSENSITIVE3/ETHYLENE INSENSITIVE3-LIKE1 reveals molecular linkage between the regulation of iron acquisition and ethylene signaling in Arabidopsis. Plant Cell **23:** 1815–1829

Ling HQ, Bauer P, Bereczky Z, Keller B, Ganal M (2002) The tomato *fer* gene encoding a bHLH protein controls iron-uptake responses in roots. Proc Natl Acad Sci USA **99:** 13938–13943

Long TA, Tsukagoshi H, Busch W, Lahner B, Salt DE, Benfey PN (2010) The bHLH transcription factor POPEYE regulates response to iron deficiency in Arabidopsis roots. Plant Cell **22:** 2219–2236

Morrissey J, Baxter IR, Lee J, Li L, Lahner B, Grotz N, Kaplan J, Salt DE, Guerinot ML (2009) The ferroportin metal efflux proteins function in iron and cobalt homeostasis in Arabidopsis. Plant Cell **21:** 3326–3338

Palmer CM, Hindt MN, Schmidt H, Clemens S, Guerinot ML (2013) MYB10 and MYB72 are required for growth under iron-limiting conditions. PLoS Genet **9:** e1003953

Ricachenevsky FK, Sperotto RA, Menguer PK, Fett JP (2010) Identification of Fe-excess-induced genes in rice shoots reveals a WRKY transcription factor responsive to Fe, drought and senescence. Mol Biol Rep **37:** 3735–3745

Robinson NJ, Procter CM, Connolly EL, Guerinot ML (1999) A ferric-chelate reductase for iron uptake from soils. Nature **397:** 694–697

Rogers EE, Guerinot ML (2002) FRD3, a member of the multidrug and toxin efflux family, controls iron deficiency responses in Arabidopsis. Plant Cell **14:** 1787–1799

Rushton PJ, Somssich IE, Ringler P, Shen QJ (2010) WRKY transcription factors. Trends Plant Sci **15:** 247–258

Schmidt W (2003) Iron solutions: acquisition strategies and signaling pathways in plants. Trends Plant Sci **8:** 188–193

Schmittgen TD, Livak KJ (2008) Analyzing real-time PCR data by the comparative C(T) method. Nat Protoc **3:** 1101–1108

Schuler M, Rellán-Álvarez R, Fink-Straube C, Abadía J, Bauer P (2012) Nicotianamine functions in the Phloem-based transport of iron to sink organs, in pollen development and pollen tube growth in Arabidopsis. Plant Cell **24:** 2380–2400

Selote D, Samira R, Matthiadis A, Gillikin JW, Long TA (2015) Iron-binding E3 ligase mediates iron response in plants by targeting basic helix-loop-helix transcription factors. Plant Physiol **167:** 273–286

Shin LJ, Lo JC, Chen GH, Callis J, Fu H, Yeh KC (2013) IRT1 degradation factor1, a ring E3 ubiquitin ligase, regulates the degradation of iron-regulated transporter1 in Arabidopsis. Plant Cell **25:** 3039–3051

Su T, Xu Q, Zhang FC, Chen Y, Li LQ, Wu WH, Chen YF (2015) WRKY42 modulates phosphate homeostasis through regulating phosphate translocation and acquisition in Arabidopsis. Plant Physiol **167:** 1579–1591

Toufighi K, Brady SM, Austin R, Ly E, Provart NJ (2005) The Botany Array Resource: e-Northerns, Expression Angling, and promoter analyses. Plant J **43:** 153–163

Ulker B, Somssich IE (2004) WRKY transcription factors: from DNA binding towards biological function. Curr Opin Plant Biol **7:** 491–498

Vert G, Grotz N, Dédaldéchamp F, Gaymard F, Guerinot ML, Briat JF, Curie C (2002) IRT1, an Arabidopsis transporter essential for iron uptake from the soil and for plant growth. Plant Cell **14:** 1223–1233

Vidal M, Legrain P (1999) Yeast forward and reverse 'n'-hybrid systems. Nucleic Acids Res **27:** 919–929

Wang H, Xu Q, Kong YH, Chen Y, Duan JY, Wu WH, Chen YF (2014) Arabidopsis WRKY45 transcription factor activates *PHOSPHATE TRANSPORTER1;1* expression in response to phosphate starvation. Plant Physiol **164:** 2020–2029

Wang HY, Klatte M, Jakoby M, Bäumlein H, Weisshaar B, Bauer P (2007) Iron deficiency-mediated stress regulation of four subgroup Ib BHLH genes in *Arabidopsis thaliana*. Planta **226:** 897–908

Wang N, Cui Y, Liu Y, Fan H, Du J, Huang Z, Yuan Y, Wu H, Ling HQ (2013) Requirement and functional redundancy of Ib subgroup bHLH proteins for iron deficiency responses and uptake in *Arabidopsis thaliana*. Mol Plant **6:** 503–513

Yang Y, Li L, Qu LJ (2016) Plant Mediator complex and its critical functions in transcription regulation. J Integr Plant Biol **58:** 106–118

Yang Y, Ou B, Zhang J, Si W, Gu H, Qin G, Qu LJ (2014) The Arabidopsis Mediator subunit MED16 regulates iron homeostasis by associating with EIN3/EIL1 through subunit MED25. Plant J **77:** 838–851

Yi Y, Guerinot ML (1996) Genetic evidence that induction of root Fe(III) chelate reductase activity is necessary for iron uptake under iron deficiency. Plant J **10:** 835–844

Yuan Y, Wu H, Wang N, Li J, Zhao W, Du J, Wang D, Ling HQ (2008) FIT interacts with AtbHLH38 and AtbHLH39 in regulating iron uptake gene expression for iron homeostasis in Arabidopsis. Cell Res **18:** 385–397